



DESY 94-131  
July 1994



**Recombination Effects  
in the Structure Function Evolution at Low  $x$ .  
Can They Be Observed at HERA?**

**K. Golec-Biernat**

*Department of Theoretical Physics, Institute of Nuclear Physics, Kraków, Poland*

**M. W. Krasny**

*L.P.N.H.E., IN2P3-CNRS, Universities Paris VI et VII, France*

*and*

*High Energy Physics Laboratory, Institute of Nuclear Physics, Kraków, Poland*

**S. Riess**

*II. Institut für Experimentalphysik, Universität Hamburg*

ISSN 0418-9833

**NOTKESTRASSE 85 - 22603 HAMBURG**

**DESY behält sich alle Rechte für den Fall der Schutzrechtserteilung und für die wirtschaftliche Verwertung der in diesem Bericht enthaltenen Informationen vor.**

**DESY reserves all rights for commercial use of information included in this report, especially in case of filing application for or grant of patents.**

**To be sure that your preprints are promptly included in the  
HIGH ENERGY PHYSICS INDEX,  
send them to (if possible by air mail):**

**DESY  
Bibliothek  
Notkestraße 85  
22603 Hamburg  
Germany**

**DESY-IfH  
Bibliothek  
Platanenallee 6  
15738 Zeuthen  
Germany**

# Recombination effects in the structure function evolution at low $x$ .

## Can they be observed at HERA?

K. Golec-Biernat

Dept. of Theoretical Physics  
Institute of Nuclear Physics  
ul Radzikowskiego 152  
31-342 Kraków, Poland

M.W. Krasny

L.P.N.H.E  
IN2P3-CNRS, Universities Paris VI et VII  
4, pl. Jussieu, T33 RdC  
75252 Paris Cedex 05, France

and  
High Energy Physics Lab., Institute of  
Nuclear Physics, PL-30055 Kraków, Poland

S. Riess

II. Institute for Experimental Physics  
University Hamburg  
Luruper Chaussee 149  
22761 Hamburg, Germany

### Abstract:

Can the non-linear QCD effects resulting from parton recombination be detected at HERA by the H1 and ZEUS detectors? We argue that an extension of the low  $x$  domain of the proton structure function  $F_2$  measurements to small electron scattering angle is essential before they can be ruled out. If, on the other hand, they are large, we find that their magnitude cannot be determined unambiguously from the measured  $Q^2$  and  $x$  dependence of  $F_2$ . This is due to large correlations between the size of recombination effects and the gluon distribution which is very weakly constrained at low  $x$  by the  $F_2$  evolution.

## 1. Introduction

The precision measurement of the deep-inelastic nucleon structure functions in the low Bjorken- $x$  region at HERA is expected to provide a novel testing ground for perturbative QCD. The rise of the structure function  $F_2$  at low  $x$ , observed by the H1 and Zeus collaborations [1], indicates that the parton recombination processes [2], expected to show up in the dense parton system, may indeed be observed and confronted with perturbative QCD predictions.

However, the present  $F_2$  measurements are not precise enough to either confirm or exclude the presence of parton recombination processes. Consequently, large ambiguities exist in the interpretation of these measurements in terms of parton densities at low  $x$ .

In this paper we address the question of whether the presently operating HERA detectors will be capable of resolving the parton recombination effects in the future. We argue that an extension of the measurement domain towards smaller values of the scattered electron angle is indispensable.

In our studies we use simulated data corresponding to our best knowledge on limits of the accuracy which can be achieved after several years of experience in measuring  $F_2$  at HERA.

We analyze these "data" using a program [3], which fits partonic distributions to  $F_2$  data using evolution equations containing parton recombination terms. This is the basic difference of our approach compared with the previous phenomenological studies of parton recombination effects [4], in which fixed parton distribution parametrizations were used.

This paper is organized as follows. In section 2 we recall the non-linear QCD evolution equations. The simulated  $F_2$  data are discussed in section 3. These data are used in the non-linear QCD fits presented in section 4 and discussed in section 5. Ambiguities in determining the gluon distribution from data are pointed out in section 6.

## 2. The evolution equations

Mueller and Qiu [5] proposed that recombination effects in the QCD evolution equations, for parton distributions should be included by adding non-linear terms to the Altarelli-Parisi equations. The form of these terms is controversial [6]. Nevertheless, it is worthwhile to test their validity with forthcoming HERA data. In this paper we use the form of these equations given in [7]:

$$Q^2 \frac{\partial [xg(x, Q^2)]}{\partial Q^2} = P_{gg} \otimes g + P_{gq} \otimes q_s - \frac{81\alpha_s^2(Q^2)}{16 R^2 Q^2} \theta(x_0 - x) \int_x^{x_0} \frac{dz}{z} \{zg(z, Q^2)\}^2 \quad (1)$$

$$Q^2 \frac{\partial [xq_s(x, Q^2)]}{\partial Q^2} = P_{qg} \otimes g + P_{qq} \otimes q_s - \frac{27\alpha_s^2(Q^2)}{160 R^2 Q^2} \theta(x_0 - x) \{xg(x, Q^2)\}^2 + \frac{\alpha_s(Q^2)}{\pi Q^2} \theta(x_0 - x) \int_x^{x_0} dz \left\{ \frac{x}{z} \gamma \left( \frac{x}{z} \right) G_H(z, Q^2) \right\}, \quad (2)$$

where  $q_s(x, Q^2)$  and  $g(x, Q^2)$  denote the sea quark and gluon distributions respectively, and  $G_H$  satisfies

$$Q^2 \frac{\partial [x G_H(x, Q^2)]}{\partial Q^2} = -\frac{81\alpha_s^2(Q^2)}{16 R^2} \theta(x_0 - x) \int_x^{x_0} dz \{x g(z, Q^2)\}^2. \quad (3)$$

The parameter  $R$ , which determines the magnitude of the non-linear terms, corresponds to a transverse size of the region within which the partons (mostly gluons) are concentrated. For  $R = 5 \text{ GeV}^{-1}$  (proton radius) partons are uniformly distributed within the proton, whereas for  $R < 5 \text{ GeV}^{-1}$  they are concentrated in clusters of smaller size ("hot spots").

The solution of eqs.(1-3) depends on two parameters:  $\Lambda_{QCD}$  and  $R$ , as well as on the form of the parton distributions at the initial scale  $Q_0^2$ .

Eq.s.(1-3) can be solved numerically. We have written a program [3], which solves the equations using the expansion of the parton densities in terms of Chebyshev polynomials. This program was used in the analysis presented below.

### 3. The simulated data

As we shall see later, the recombination effects represented by the non-linear terms in eqs.(1-3) cannot be identified using recently published H1 and Zeus  $F_2$  data [1]. This is due both to the limited acceptance of the detectors in the low  $x$  region and to a large systematic uncertainty of the measurements. The limited angular coverage of the H1 and ZEUS detectors for measuring deep inelastically scattered electrons ( $\theta_e \geq 7.5^\circ$ ) restricts severely the small  $x$  domain, where the non-linear terms of eqs.(1-3) are expected to be important. In addition, the substantial photoproduction background restricts the available  $y$  range of the measurement to  $y \leq 0.6$ .

The measurement domain might be extended towards very small  $x$ , of the order  $10^{-5}$ , in a dedicated low- $x$  experiment. If the HERMES electron spectrometer [8] were used in a colliding mode, in which 30 GeV electrons were scattered off 820 GeV protons accelerated at HERA, a precision measurement of  $F_2$  in this  $x$  region would be possible [9] by extending the  $\theta_e$  domain down to  $\theta_e \approx 3^\circ$ .

Can the recombination effects be resolved if such dedicated measurement is made? To answer this question we have considered two distinct scenarios of the size of recombination effects and simulated the measurement of the two corresponding  $F_2$  data sets in the angular domain of  $\theta_e > 3^\circ$  and  $Q^2 \geq 2 \text{ GeV}^2$ . The first data set, called hereafter  $R_{\infty}$ , was simulated according to eqs.(1-3) with the non-linear terms omitted (the  $R$  parameter was set to infinity) while the second, called hereafter  $R_3$ , corresponds to the  $R$  parameter set to  $3 \text{ GeV}^{-1}$ . We then examine if we can unambiguously identify the effects which we have put in from the results of the QCD fits to these two data sets. The simulated data correspond to an integrated luminosity of  $10 \text{ pb}^{-1}$ , and to our best knowledge of the limits of systematic accuracy which might be achieved after several years of experience in measuring  $F_2$ .

Both data sets were generated to be compatible with the data published by H1 and ZEUS in the region accessible by the experiments (Figs. 1a and 1b). The error bars are taken to be the anticipated statistical and systematic errors added in quadrature. The systematic errors include an uncertainty in the measured scattered electron momentum and its angle. They are in the range between 5-10 %.

### 4. The QCD fits

To see if the simulated recombination effects can be unambiguously detected, we performed QCD fits to the two data sets using eqs.(1-3). The  $\chi^2$  of the fits is defined as the following sum over measured points

$$\chi^2 = \sum_i \frac{(F_2^{\text{exp}}(x_i, Q_i^2) - F_2^{\text{fit}}(x_i, Q_i^2))^2}{\sigma_{i,\text{sys}}^2 + \sigma_{i,\text{stat}}^2}, \quad (4)$$

where  $F_2^{\text{exp}}$  and  $F_2^{\text{fit}}$  are experimental (simulated) and calculated proton structure functions respectively, and  $\sigma_{i,\text{sys}}^2$  and  $\sigma_{i,\text{stat}}^2$  are the systematic and statistical errors.

The  $\chi^2$  was minimized with respect to the fit parameters using the MINUIT package [10]. The following general form, motivated by the phenomenological studies in the small  $x$  region [7], was assumed for the  $x$  dependence of the gluon and sea quark distributions at  $Q_0^2 = 4 \text{ GeV}^2$ :

$$xg(x) = (A_g x^{-\lambda_g} + B_g) W_g(x) \quad (5)$$

$$xq_s(x) = (A_s x^{-\lambda_s} + B_s) W_s(x). \quad (6)$$

$W_{g,s}(x)$  are polynomials whose parameters are not sensitive to the small  $x$  behavior of the parton densities. Only the parameters  $\lambda, A, B$  are important in the small  $x$  region, and they were fitted.

For simplicity, the magnitude of the  $R$  and  $\Lambda_{QCD}$  parameters were fixed in all fits.  $\Lambda_{QCD}$  was taken to be  $200 \text{ MeV}$  (for 4 flavors), which is an average value obtained from the leading log analysis of fixed target DIS experiments [11]. Three values of  $R$  were assumed,  $R = 3, 5, \infty \text{ GeV}^{-1}$ . For each minimization step, the momentum sum rule was imposed. We performed the fits for two values of the angular cut-off of  $\theta_e \geq 3^\circ$  and  $\theta_e \geq 7.5^\circ$ , corresponding to the two detector configurations mentioned above. In all fits the leading log approximation for the linear part of eqs.(1-3) was used.

As a basic consistency check of our procedure, we verified that for each simulated data set we find the parameter values assumed in the data simulation, i.e. a fit to the  $R_{\infty}$  data set leads to a very large value of  $R$ , and a fit to  $R_3$  data set finds  $R = 3 \text{ GeV}^{-1}$ . The results of these fits are presented in Fig.1.

### 5. The recombination effects

In this section we shall interpret the simulated  $F_2$  data by analysing the results of the fits explained in the previous section. Since we know the underlying physics picture of the simulated data sets we can verify if our interpretation is correct and unambiguous.

From the fitted  $F_2$  we extract the logarithmic slopes  $\partial F_2 / \partial \log(Q^2)$  for different  $x$  values, and compare them for a compact illustration of the fit quality to the logarithmic slopes of the simulated structure function  $F_2$ . The results are shown in Fig. 2.

Figure 2a shows the slopes for  $R_{\infty}$  data set simulated with the minimal detection angle  $\theta_e > 7.5^\circ$ . Three independent fits to these data were performed: the standard fit with the linear Altarelli-Parisi equations ( $R = \infty$  in eqs.(1-3)), and with the parameter  $R$  set to  $R = 5$  and  $3 \text{ GeV}^{-1}$  in the fits. In all cases acceptable  $\chi^2$  values are obtained ( $\chi^2/NDF =$

(80, 71, 79)/74 respectively). Thus, we conclude that the present HERA experiments can not resolve the recombination effects corresponding to  $R = 5$  and  $3 \text{ GeV}^{-1}$ .

Extending the electron detection angle to  $\theta_e > 3^\circ$ , and therefore measuring smaller values of  $x$  changes the picture considerably as shown in Fig. 2b. Again fits with  $R$  set to  $3, 5, \infty \text{ GeV}^{-1}$  were made to the  $R_{\infty}$  data set, but simulated now down to  $\theta_e = 3^\circ$ . The fit with the linear evolution equations ( $R = \infty$ ) describes the data well ( $\chi^2/NDF = 106/118$ ) while the  $R = 5$  and  $R = 3$  fits yield unacceptable  $\chi^2/NDF$  of 160/118 and 293/118 respectively. Thus, we fail to obtain acceptable fits for the  $R = \infty$  data set using non-linear evolution equations with  $R \leq 5 \text{ GeV}^{-1}$ .

We now reverse the problem and ask if the recombination effects present in the  $R_3$  data set can be correctly identified. Figure 2c shows the slopes derived from the fits to the  $R_3$  data set. Again the larger angular coverage is considered. All three fits, with  $R = 3, 5, \infty \text{ GeV}^{-1}$ , describe this data set equally well ( $\chi^2/NDF = (102, 118, 104/118)$  respectively). As a consequence, if recombination effects are present in the data they can not be ambiguously detected.

Summarizing, the recombination effects, of the form specified by eqs.(1-3), can be ruled out if they do not exist in the HERA  $x$  domain. If they exist their presence could not be confirmed nor their magnitude determined.

## 6. The gluon distribution at low $x$

We now examine to which extent the gluon distribution can be constrained at low  $x$  if we allow the recombination terms to be present in the evolution equations.

In fig 3a and 3b we show the gluon distributions at  $Q^2 = 4$  and  $Q^2 = 40$  obtained from the fits of: the linear part of eqs.(1-3) to the  $R_{\infty}$  data set (solid line), the linear part of the eqs.(1-3) to the  $R_3$  data set (dashed line), complete eqs.(1-3) with  $R = 3 \text{ GeV}^{-1}$  to the  $R_3$  data set (dotted line).

All fits are of equally good quality. The resulting gluon distributions differ, however, as shown in fig 3. These distributions illustrate the uncertainty range of the gluon distribution due to shadowing terms of eqs.(1-3). This uncertainty is particularly large at low  $Q^2$  and, as expected, decreases at large  $Q^2$  where the recombination effects are smaller. The three gluon distributions behave at  $Q^2 = 4 \text{ GeV}^2$  as  $x^{-0.5}$ ,  $x^{-0.25}$  and  $x^{0.0}$  respectively at small  $x$ .

The above analysis indicates clearly that pinning down experimentally the size of recombination effects is necessary to determine the gluon distribution at low  $x$  from the scaling violation of  $F_2$  only.

As our two data sets are compatible with the  $F_2$  data of H1 and ZEUS the above uncertainty is present in the gluon distribution presented in [12].

## 7. Conclusions

To rule out the presence of the non-linear terms in the QCD evolution equations for the proton structure function  $F_2$  which describe the recombination of partons at low  $x$ , we have demonstrated that it is necessary at HERA to detect electrons at smaller scattering

angle (below  $7.5^\circ$ ) to be sensitive to recombination of partons clustering on a distance scale  $R \leq 5 \text{ GeV}^{-1}$ . This could possibly be achieved by means of a precision electron spectrometer, similar to that under construction for the HERMES experiment at HERA but run in colliding mode with  $820 \text{ GeV}$  protons rather than a gas jet target.

If clustering and recombination effects are important at HERA, and if they are described by the non-linear parts of eqs.(1-3), then their manifestation in  $F_2$  measurements may be mimicked by a suitable choice of the gluon distribution parametrisation at fixed  $Q^2$  and conventional linear evolution. Thus, it is essential to measure the gluon distribution by other independent means such as from measurements of  $\sigma_L/\sigma_T$ , heavy quark production or jet production, if clustering and recombination effects are to be observed unambiguously at HERA.

This analysis has assumed that a leading logarithm approximation is valid for the linear part of eqs.(1-3). Any modifications to these conclusions by making a next-to-leading logarithm approximation and by replacing protons in the HERA storage rings by heavy ions will be reported in separate papers.

## Acknowledgements

We are grateful to Jochen Bartels, Dieter Haidt and in particular to John Dainton for critical reading of the manuscript.

## References

- [1] H1 Collaboration (I.Abt, et al.), Nucl.Phys. **B407** (1993) 515; ZEUS Collaboration (M.Derrick, et al.), Phys.Lett. **B306** (1993) 412.
- [2] L.N.Gribov, E.M.Levin, M.G.Ryskin, Phys.Rep.**100** (1983) 1.
- [3] K.Golec-Biernat, M.W.Krasny, S.Riess, FITEQ-Users Guide (*in preparation*).
- [4] J.Bartels, K.Charchula, J.Feltesse, Proceedings of the Workshop "Physics at Hera", Hamburg 1991, p.193; A.Altman, M.Gluck, E.Reya, Phys.Lett. **B285** (1992) 359.
- [5] A.H.Mueller, J.Qiu, Nucl.Phys. **B268** (1986) 427.
- [6] J. Bartels, M.G. Ryskin, Z. Phys **C60** (1993) 751.
- [7] J. Kwieciński, A.D.Martin, W.J.Stirling and R.G.Roberts, **D42** (1990) 3645.
- [8] HERMES Collaboration, *Technical Design Report*, DESY, 1993.
- [9] M.W.Krasny, *Saclay Note*, Nov. 1991, unpublished.
- [10] F.James, M.Roos, MINUIT-Users Guide, Program Library D506, CERN, 1981.
- [11] BCDMS Collaboration (A.C.Benvenuti, et al.), Phys.Lett. **B223** (1989) 490.
- [12] H1 Collaboration (I.Abt, et al.), Phys.Lett. **B321** (1993) 161.

## Figure Captions

Fig. 1

Comparison of simulated (open circles)  $R_\infty$  (a), and  $R_3$  (b) data on  $F_2$  (for the description see chapter 3) to the measured  $F_2$  structure function of H1 (squares) and ZEUS (triangles) [1]. The solid lines represent  $R = \infty$  fit, while dashed lines  $R = 3$  fit, respectively, to  $R_\infty$  and  $R_3$  simulated data sets. Note that only the low  $x$  simulated data are shown. Higher  $x$  data points, not shown in the figure, were also used in the fits.

Fig. 2

The  $F_2$  logarithmic slopes  $\partial F_2 / \partial \log(Q^2)$  as a function of  $x$ . The open points represent the values calculated for the  $R_\infty$  data set in the domain of  $\theta_e > 7.5^\circ$  (a) and  $\theta_e > 3^\circ$  (b), and the values calculated for the  $R_3$  data set in the domain of  $\theta_e > 3^\circ$  (c). The solid, dashed and dotted lines are derived from the results of the  $R = \infty, 5, 3 \text{ GeV}^2$  fits respectively.

Fig. 3

The gluon distribution  $xG(x)$  resulting from the fits: at  $Q^2 = 4 \text{ GeV}^2$  (a), and  $Q^2 = 40 \text{ GeV}^2$  (b). The solid lines represent  $R = \infty$  fit to the  $R_\infty$  data set, the dashed lines represent  $R = \infty$  fit to the  $R_3$  data set, and the dotted lines represent  $R = 3$  fit to the  $R_3$  data set simulated in the  $\theta_e > 3^\circ$  region.

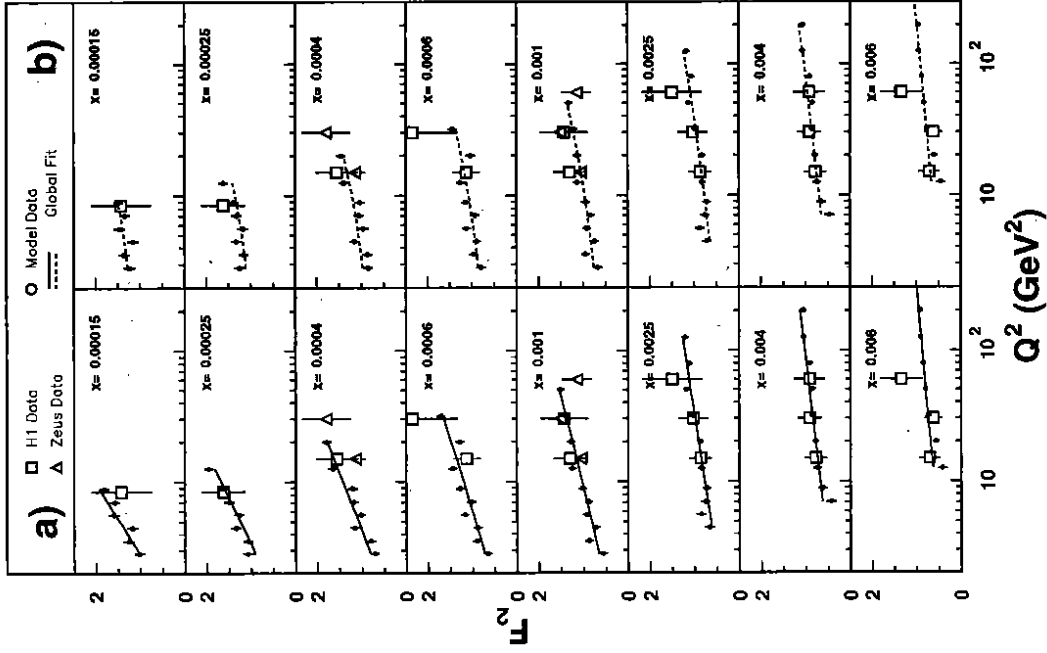


Figure 1:

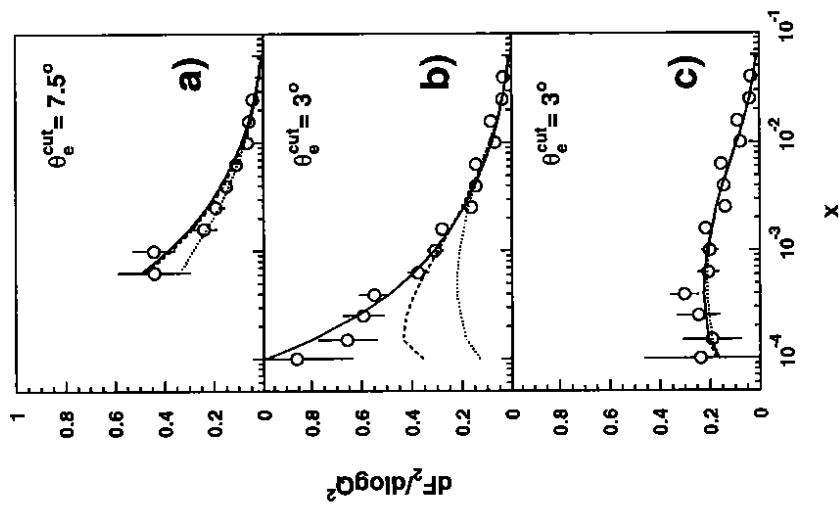


Figure 2:

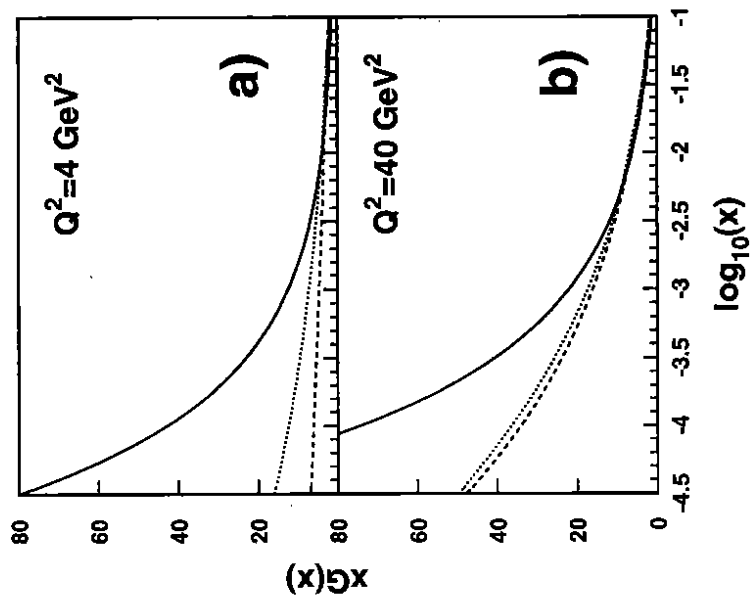


Figure 3: